

Determination of susceptibility and specific heat critical exponents for weak itinerant-electron ferromagnets from vibrating reed experiments

K. Balakrishnan and S. N. Kaul*

School of Physics, University of Hyderabad, Central University P.O., Hyderabad 500 046, Andhra Pradesh, India

(Received 10 July 2001; revised manuscript received 30 October 2001; published 19 March 2002)

We report the observation of a *linear* relationship between the magnetic contribution to Young's modulus, $\Delta E/E_0$, and inverse magnetic susceptibility χ^{-1} for amorphous weak itinerant-electron ferromagnets $\text{Fe}_{90}\text{Zr}_{10}$ and $\text{Fe}_{91}\text{Zr}_9$ in the asymptotic critical region near the ferromagnetic-paramagnetic phase transition. The proportionality $\Delta E(T)/E_0 \propto \chi^{-1}(T)$ is shown to provide as accurate a means of determining the *asymptotic* critical exponent γ and the leading "correction-to-scaling" amplitudes for susceptibility from the $\Delta E/E_0$ data as a *direct* measurement of magnetic susceptibility does. Similarly, the well-known relation between the magnetic contributions to sound velocity and specific heat is fully exploited to extract accurate estimates for the *universal* critical amplitude ratio A^+/A^- and the asymptotic critical exponents α^\pm for the specific heat from the sound velocity data. The presently determined values of α^\pm and γ , together with the reported value for spontaneous magnetization critical exponent β , not only obey the scaling equalities $\alpha^+ = \alpha^-$ and $\alpha + 2\beta + \gamma = 2$ but also assert that the atomic magnetic moments in the alloys in question interact with one another through an *attractive* interaction which *decays faster* than $1/r^5$ with the interatomic spacing, r .

DOI: 10.1103/PhysRevB.65.134412

PACS number(s): 75.40.Cx, 64.60.Fr, 72.55.+s, 75.50.Kj

I. INTRODUCTION

Investigation of acoustic properties has played an important role in characterizing the critical behavior^{1,2} of a wide variety of systems near phase transitions of different kind. While low-frequency acoustic velocity data provide useful information about the equilibrium properties, static critical phenomena, and spin-acoustic phonon coupling, ultrasonic attenuation measurements determine the dynamic behavior, characteristic relaxation times, and relaxation mechanisms. Early studies have mainly concentrated^{1,3} on the anomaly in sound-wave attenuation at the critical point and on the attendant frequency dispersion or relaxation. With the realization that the sound velocity in the low-frequency limit does not involve relaxation effects, which complicate the interpretation of results in the case of sound attenuation, the focus has lately shifted to the investigation of changes in sound velocity near the phase transition. Added motivation for pursuing this type of study in magnetic systems, in particular, is provided by (i) a well-established³⁻⁸ direct relationship between the magnetic contribution to specific heat, C_M , and the relative change in sound velocity, $\Delta V/V_0$, due to critical spin-fluctuation-phonon scattering, i.e., $\Delta V/V_0 \propto -C_M$, in the critical region, (ii) extremely high resolution achieved in sound velocity experiments than in specific heat measurements, and (iii) the availability of accurate theoretical estimates^{9,10} for the *asymptotic* critical exponents that characterize different universality classes of *static* critical point phenomena. Thus the sound velocity measurements on insulating (localized-electron) ferromagnets^{3,4} and antiferromagnets^{3,5} and even metallic spin glasses⁸ have been used to determine the critical exponent α^- (α^+) that characterizes the thermal critical behavior of specific heat near the magnetic order-disorder phase transition as the critical point T_C is approached from below (above). Mostly, the

value of either α^- or α^+ has been extracted^{3,4,8} from the sound velocity data; in rare cases where both critical exponents⁵ have been determined, the exponent values *do not obey*⁵ the scaling equality $\alpha^- = \alpha^+$. Moreover, a large scatter in the reported^{3-5,8} exponent values precludes a meaningful comparison between theory and experiment. A total neglect of the "correction-to-scaling" terms in the theoretical expression used to fit the sound velocity data and/or a sizable uncertainty in the estimation of the nonmagnetic background seem to be the root causes. The sound velocity studies carried out hitherto have, therefore, proved inconclusive.

With a view to remedy this situation and to exploit the full potential of the sound propagation technique in unraveling the exact nature of the singularity at T_C , a detailed magnetoelastic investigation of the critical behavior of *well-characterized*^{11,12} weak itinerant-electron ferromagnets, amorphous $(a-x)\text{Fe}_{90}\text{Zr}_{10}$ and $\text{Fe}_{91}\text{Zr}_9$ alloys, has been undertaken. Considerations that led to the above choice of samples for the type of study intended are as follows. (i) $a\text{-Fe}_{90+x}\text{Zr}_{10-x}$ ($x=0, \pm 1, \pm 2$) alloys exhibit Invar behavior¹³ and weak itinerant-electron ferromagnetism^{12,14,15}; no Young's modulus, $E(T)$, or sound velocity, $V(T)$, data in the critical region are presently available on weak itinerant-electron ferromagnets. (ii) The spin-phonon interaction responsible for the critical anomaly in sound propagation arises in most cases via the strain modulation of the exchange interaction (volume magnetostrictive coupling). Now that the above-mentioned compositions in the $a\text{-FeZr}$ alloy series possess large volume magnetostriction,^{13,16} the anomaly in $V(T)$ at T_C is expected to be pronounced and hence easily detectable in these samples. (iii) Earlier attempts to determine the specific heat critical exponents α^- and α^+ from electrical resistivity measurements on the amorphous alloys in question have failed¹¹ because of the large nonsingular contribution arising mainly from the scattering of conduction electrons from disordered structure.

II. EXPERIMENTAL DETAILS

Vibrating reed experiments have been performed on *stress-relieved* (at 100 °C for 14 days) absolutely flat ribbon strips (length 10–15 mm, width 2 mm and thickness ~ 0.03 mm), which form the reed, of a -Fe₉₀Zr₁₀ and a -Fe₉₁Zr₉ alloys at 100 mK steps in the critical region near the ferromagnetic- (FM-) paramagnetic (PM) phase transition and at larger temperature intervals outside the critical regime, covering as wide a temperature as $80\text{K} \leq T \leq 350\text{K}$. Details about the sample preparation-cum-characterization and the vibrating reed experimental setup are given in our earlier publications.^{11,12,17} In these experiments, the fundamental (resonance) vibration frequency $f = (d/4\pi\sqrt{3}) \times (1.875/l)^2 V$ (where V is the sound velocity while d and l are the thickness and length of the ribbon strip) of the sample reed is measured at different temperatures. Young's modulus E is related to the sound velocity V as $V = \sqrt{E/\rho}$, where ρ is the mass density. In order to arrive at the true values of V and E at different temperatures, the density and temperature variations of the measured resonance frequency f_{meas} are corrected for the temperature-dependent thermal expansion coefficient $\alpha(T)$ using the relations¹⁸ $V(T) \propto f_{meas}(T)[1 + \alpha(T)\Delta T] = f_{corr}(T)$ and $E(T) \propto f_{meas}^2(T)[1 - \alpha(T)\Delta T] = f_{corr}^2(T)$, where ΔT is the change in temperature from the *reference* temperature ($\approx T_C$, the Curie temperature) at which α changes sign.

Estimation of the magnetic contribution to the sound velocity V or Young's modulus E requires the subtraction of the nonmagnetic contribution to V or E (henceforth referred to as the *background* contribution), arising from the anharmonic terms in the interatomic potential, from the measured $V(T)$ or $E(T)$ data. To accurately determine the background contribution $f_{bg}(T)$ or $f_{bg}^2(T)$, the *corrected* resonance frequency, $f_{corr}(T)$, or frequency squared, $f_{corr}^2(T)$, data are fitted to the expression $\mathcal{F}(T) = \mathcal{F}(0) - A/(e^{\Theta_E/T} - 1)$, derived by Varshni,¹⁹ where $\mathcal{F}(T)$ stands for $f_{corr}(T)$ or $f_{corr}^2(T)$, for temperatures well above T_C using a "range-of-fit" analysis. In this analysis, the values of the fitting parameters $\mathcal{F}(0)$, A , and Einstein temperature, Θ_E , and the sum of the deviation squares are monitored as the fit range $T_{min} \leq T \leq T_{max}$ is varied by keeping T_{max} fixed at the highest temperature value and raising T_{min} towards T_{max} by progressively leaving out of the analysis the data taken at $T \leq T_{min}$. The temperature range over which the values of the fitting parameters *do not change* upon variation of T_{min} is 270–350 K (270–320 K) for a -Fe₉₀Zr₁₀ (a -Fe₉₁Zr₉). With the parameter values so obtained, f_{bg} or f_{bg}^2 is calculated as a function of temperature down to the lowest temperature $\sim 80\text{K}$ using Varshni's expression. The resulting variations of f_{bg} with temperature and the measured resonance frequency data *corrected* for thermal expansion, $f_{corr}(T)$ are depicted in Fig. 1 and denoted by solid curves and symbols (open circles for a -Fe₉₀Zr₁₀ and open triangles for a -Fe₉₁Zr₉), respectively. The data presented in Fig. 1 are also representative of the $f_{bg}^2(T)$ and $f_{corr}^2(T)$ data. More details about the determination of $f_{corr}(T)$ and $f_{bg}(T)$ are given elsewhere.¹⁸ The fractional *magnetic* contributions to the sound velocity,

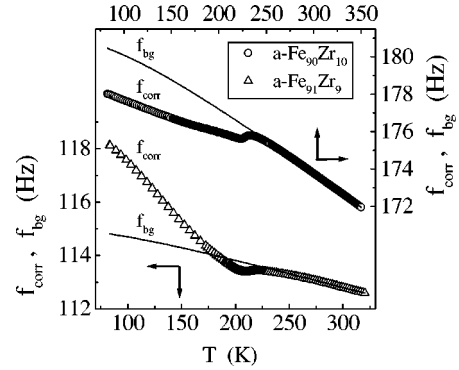


FIG. 1. Temperature variation of the nonmagnetic part of the resonance frequency f_{bg} (solid curves) and the measured resonance frequency corrected for thermal expansion, f_{corr} , for a -Fe₉₀Zr₁₀ (open circles) and a -Fe₉₁Zr₉ (open triangles) alloys.

$\Delta V(T)/V_0 = [V(T) - V_{bg}(T)]/V_{bg}(T_0)$, and Young's modulus, $\Delta E(T)/E_0 = [E(T) - E_{bg}(T)]/E_{bg}(T_0)$, shown in Figs. 2 and 3, are accurately (relative accuracy better than 10 ppm) determined from the equalities $\Delta V(T)/V_0 = [f_{corr}(T) - f_{bg}(T)]/f_{bg}(T_0)$ and $\Delta E(T)/E_0 = [f_{corr}^2(T) - f_{bg}^2(T)]/f_{bg}^2(T_0)$, where $T_0 = 273.15$ K is the ice point (reference temperature). Note that in Fig. 2, $\Delta V(T)/V_0$ is plotted against the reduced temperature $\epsilon = (T - T_C)/T_C$ rather than against T to facilitate comparison with theory.

III. DATA ANALYSIS, RESULTS, AND DISCUSSION

Figure 4 displays the $\Delta V/V_0$ data in a narrow temperature range around T_C . As already stated in the Introduction, it is customary to extract specific heat critical exponents α^- and

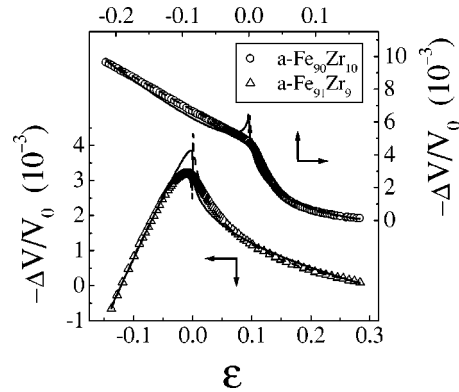


FIG. 2. Temperature variation of $\Delta V/V_0$ over a wide temperature range embracing the critical region. Solid and dashed curves represent the least-squares fits to the $\Delta V/V_0$ data for a -Fe₉₀Zr₁₀ (open circles) and a -Fe₉₁Zr₉ (open triangles) based on Eq. (6) of the text. For details about the different types of fits, see text. By giving equal weightage to the data within and outside the asymptotic critical region, these fits achieve at best a good overall agreement with the data. However, the corresponding fit parameters have unphysically large values, which are substantially different from those that reproduce the observed temperature variations within the asymptotic critical region (Fig. 4). Consequently, such fits deviate considerably from the data particularly in the vicinity of $\epsilon = 0$.

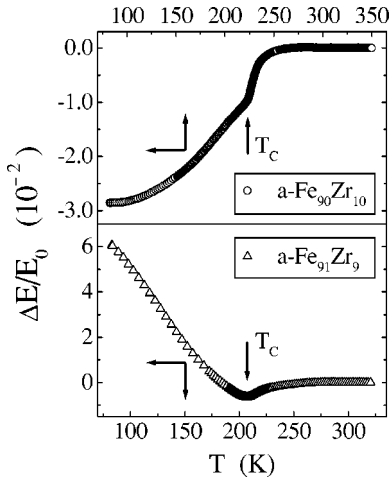


FIG. 3. Fractional *magnetic* contribution to Young's modulus, $\Delta E/E_0$, as a function of temperature for the *a*-Fe₉₀Zr₁₀ (open circles) and *a*-Fe₉₁Zr₉ (open triangles) alloys. The arrows indicate the Curie temperature T_C .

α^+ from the sound velocity data by making use of the *direct proportionality*³⁻⁸ between the magnetic contributions to the specific heat, $C_M(T)$, and sound velocity, $\Delta V/V_0$. Such a proportionality is strictly valid when the transition at T_C is sharp. When this condition is not met, i.e., when the transition is not sharp, the full thermodynamic relationship between $\Delta V/V_0$ and C_M has to be used. A brief derivation of this relationship is furnished below.

Consider the form³ of free energy

$$F = F_0(v, T) + Tf(T/T_C), \quad (1)$$

where the first and second terms, respectively, represent the elastic (nonmagnetic) and magnetic components. In Eq. (1), the Curie temperature T_C (a direct measure of the strength of exchange interactions coupling the spins in the system) is a *function* of only the volume v . Using the thermodynamic

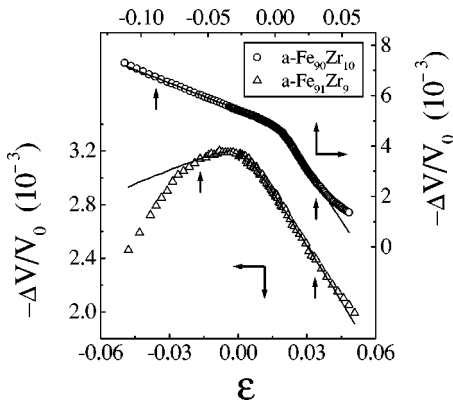


FIG. 4. $\Delta V/V_0$ as a function of reduced temperature $\epsilon = (T - T_C)/T_C$. The solid curves depict the least-squares fits to the $\Delta V/V_0$ data based on Eq. (6) of the text for the *a*-Fe₉₀Zr₁₀ (open circles) and *a*-Fe₉₁Zr₉ (open triangles) alloys. The upward arrows indicate the temperatures that mark the upper bounds of the asymptotic critical region and beyond which the data start deviating from the fits.

relations $B_T = v(\partial^2 F / \partial v^2)_T$, $S_v = -(\partial F / \partial T)_v$ and $C_v = -T(\partial^2 F / \partial T^2)_v$ for the *total* isothermal bulk modulus, entropy, and specific heat at constant volume, Eq. (1) yields the magnetic contribution to bulk modulus, B_M , in terms of the magnetic contributions to entropy, S_M , and specific heat, C_M , in the critical region, as

$$B_M = B_T - B_0 = -v(\partial^2 T_C / \partial v^2)S_M - v(1/T_C) \times (\partial T_C / \partial v)^2 C_M, \quad (2)$$

with

$$S_M = S_v - S_0 = -[f(T/T_C) + (T/T_C)(\partial f / \partial T)_v], \quad (3)$$

$$C_M = C_v - C_0 = -T[(2/T_C)(\partial f / \partial T)_v + (T/T_C^2)(\partial^2 f / \partial T^2)_v], \quad (4)$$

where $B_0 = v(\partial^2 F_0 / \partial v^2)_T$, $S_0 = -(\partial F_0 / \partial T)_v$, and $C_0 = -T(\partial^2 F_0 / \partial T^2)_v$. From Eq. (2), it follows that the fractional *magnetic* contribution to the sound velocity is given by

$$\Delta V/V_0 = (B_T - B_0)/2B_0 = -(v/2B_0)[(\partial^2 T_C / \partial v^2)S_M + (1/T_C)(\partial T_C / \partial v)^2 C_M]. \quad (5)$$

Equation (5) contains contributions from both first- and second-order derivatives of T_C with respect to volume or, equivalently, from both first- and second-order derivatives of exchange coupling with respect to strain.⁷ *Singular* and *non-singular* contributions to $\Delta V(T)/V_0$ at T_C originate from terms involving $C_M(T)$ and $S_M(T)$, respectively. The sharpness of the *negative* cusp at T_C in $\Delta V(T)/V_0$ is determined by the relative magnitude of these contributions; i.e., the cusp at T_C is sharp when the singular term *dominates* over the nonsingular one [e.g., when $(\partial T_C / \partial v)^2 / T_C \gg (\partial^2 T_C / \partial v^2)$] whereas the anomaly at T_C is not pronounced if the reverse is true. In the former case, the relation (5) permits an *indirect* but accurate determination of the specific heat *asymptotic* critical amplitudes (exponents) A^\pm (α^\pm) and “correction-to-scaling” amplitudes (exponents) $a_{c_1}^\pm$, $a_{c_2}^\pm$ (Δ_1 , Δ_2) [cf. Eq. (6)] from the $\Delta V(T)/V_0$ data.

An elaborate “range-of-fit” analysis^{12,20} of the $\Delta V/V_0$ data has been carried out based on the general expression^{8,20}

$$-\Delta V/V_0 = (A^\pm / \alpha^\pm) |\epsilon|^{-\alpha^\pm} [1 + a_{c_1}^\pm \alpha^\pm |\epsilon|^{\Delta_1} + a_{c_2}^\pm \alpha^\pm |\epsilon|^{\Delta_2}] - (A^\pm / \alpha^\pm) + B^\pm + \hat{A}^\pm (\pm \epsilon), \quad (6)$$

where $\epsilon = (T - T_C)/T_C$, the plus and minus signs denote temperatures above and below T_C , the last two terms represent the nonsingular background [the first term in Eq. (5)], the remaining terms constitute the singular contribution [the second term in Eq. (5)], and A^\pm ($a_{c_1}^\pm$, $a_{c_2}^\pm$) and α^\pm (Δ_1 , Δ_2) are the *asymptotic* (leading correction-to-scaling) critical amplitudes and critical exponents, respectively. At first, the $\Delta V(T)/V_0$ data for $T < T_C$ and $T > T_C$ are *separately* fitted to a single power law (SPL) by setting $a_{c_1}^\pm = a_{c_2}^\pm = 0$ in Eq. (6) and the range-of-fit analysis^{12,20} is used to monitor the change, if any, in the values of the fitting parameters A^\pm , α^\pm , B^\pm , \hat{A}^\pm , and T_C^\pm as the temperature range ($|\epsilon_{\min}|$

TABLE I. Parameter values pertaining to Eq. (6) of the text. $\mathfrak{R}=[B^+-(A^+/\alpha^+)][B^-(A^-/\alpha^-)]$.

Parameters	$a\text{-Fe}_{90}\text{Zr}_{10}$	$a\text{-Fe}_{91}\text{Zr}_9$	Theory
			$d=3$ Heisenberg model ^a
Fit range $\epsilon < 0$ ($10^3 \epsilon$)	$-89 \leq \epsilon \leq -0.39$	$-48 \leq \epsilon \leq -0.95$	
Fit range $\epsilon > 0$ ($10^3 \epsilon$)	$+0.42 \leq \epsilon \leq +33$	$+0.26 \leq \epsilon \leq +34$	
$T_C^- = T_C^+$ (K)	223.066(5)	208.097(8)	
$\alpha^- = \alpha^+$	-0.115(5)	-0.115(5)	-0.115(9)
A^+ (10^{-5})	-10.3(3)	-9.5(2)	
A^- (10^{-5})	-6.5(7)	-6.16(8)	
A_1^+ (10^{-5})	-8.24(1)	-2.95(1)	
A_1^- (10^{-2})	2.00(1)	-0.80(1)	
B^+ (10^{-3})	5.36(1)	3.65(1)	
B^- (10^{-3})	5.068(1)	3.479(1)	
\mathfrak{R}	0.99(1)	0.96(4)	
A^+/A^-	1.55(3)	1.54(4)	1.55(3)

^aReferences 9, 10, and 22.

$\leq |\epsilon| \leq |\epsilon_{\max}|$) of the fit is narrowed down by raising (lowering) $|\epsilon_{\min}|$ ($|\epsilon_{\max}|$) towards $|\epsilon_{\max}|$ ($|\epsilon_{\min}|$) while keeping $|\epsilon_{\max}|$ ($|\epsilon_{\min}|$) fixed at a given value. The optimum values of the fitting parameters and the fit ranges over which they remain stable are displayed in Table I. The salient features (Table I) that emerge are as follows. (i) $T_C^- = T_C^+$ and $\alpha^- = \alpha^+$ within the uncertainty limits. (ii) The (universal) amplitude ratio $A^+/A^- \approx 1.55$ regardless of the alloy composition. (iii) As dictated by the requirement that, for $\alpha < 0$, $\Delta V^+/V_0 = \Delta V^-/V_0$ at $T = T_C$, the parameter values satisfy the equality $B^+ - (A^+/\alpha^+) = B^- - (A^-/\alpha^-)$ within the error limits. (iv) While the term $(A^\pm/\alpha^\pm)|\epsilon|^{-\alpha^\pm}$ in Eq. (6) is mainly responsible for the singularity in $\Delta V(T)/V_0$ at $T = T_C$, the term linear in ϵ [i.e., the last term in Eq. (6)] governs the temperature dependence of $\Delta V/V_0$ in the critical region except for temperatures in the immediate vicinity of T_C . Next, the range-of-fit analysis is carried out using the full expression (6), which includes the leading correction-to-scaling terms. The agreement between the theory and experiment is optimized by varying the parameters A^\pm , α^\pm , B^\pm , \hat{A}^\pm , $a_{c_1}^\pm$, $a_{c_2}^\pm$, and T_C^\pm while keeping Δ_1 and Δ_2 fixed at the theoretically predicted^{9,10,21} estimates of $\Delta_1 = 0.11$ and $\Delta_2 = 0.55$. The main outcome of this exercise is that the quality of the theoretical fits and the values of all the SPL fitting parameters, listed in Table I, remain essentially unaltered. This is so because the coefficients of the leading correction-to-scaling terms, i.e., $a_{c_1}^\pm$ and $a_{c_2}^\pm$, possess negligibly small values. The optimum SPL fits to the $\Delta V/V_0$ data (open symbols) are depicted by the solid curves and the extent (width) of the asymptotic critical region (ACR) is indicated by upward arrows in Fig. 4. Moreover, the presently determined values for the critical exponents α^\pm and the universal amplitude ratio A^+/A^- conform very well with those theoretically predicted^{9,10,22} for a three-dimensional isotropic nearest-neighbor Heisenberg ferromagnet, i.e., for a *pure* (ordered) spin system with space dimensionality $d=3$ and spin dimensionality $n=3$; see Table I.

When the $\Delta V/V_0$ data over a wide temperature range are fitted (dashed curves in Fig. 2) separately for temperatures above and below T_C to the modified version of Eq. (6), in which $a_{c_1}^\pm$ and $a_{c_2}^\pm$ are set equal to zero, with T_C^\pm fixed at the values determined in the ACR, good overall fits are obtained for $T < T_C$ and $T > T_C$, except for temperatures in the ACR, with $\alpha^+ \approx \alpha^- = -0.26(2)$ and $-0.33(2)$ for $a\text{-Fe}_{90}\text{Zr}_{10}$ and $a\text{-Fe}_{91}\text{Zr}_9$, respectively, but $[B^+ - (A^+/\alpha^+)] \approx 2 [B^- - (A^-/\alpha^-)]$. If the $\Delta V/V_0$ data are fitted over the entire temperature range $T_{\min} < T_C < T_{\max}$ with the constraint $[B^+ - (A^+/\alpha^+)] = [B^- - (A^-/\alpha^-)]$ imposed and the exponents α^+ and α^- fixed at the values obtained from the individual fits above and below T_C , the quality of the fit (solid curves in Fig. 2) worsens, as is clearly noticed in Fig. 2. From the results of the different types of fits to the $\Delta V/V_0$ data attempted based on Eq. (6), we conclude that the magnitudes of the critical exponents α^\pm and critical amplitude ratio A^+/A^- listed in Table I are their true *asymptotic* values.

A *mean-field* treatment²³ of the electron-electron (Coulomb plus exchange), phonon-phonon, and electron-phonon interactions in itinerant-electron ferromagnets yields the following expression for the magnetic contribution to sound velocity (hence to the Young's modulus) in the *paramagnetic* state:

$$\Delta E(T)/E_0 = (V/V_0)^2 - 1 = (\xi - 1) + [(\chi_P/\chi_S(T))]. \quad (7)$$

In Eq. (7), V_0 is the Bohm-Staver sound velocity of the itinerant-electron system in the absence of exchange interaction (the so-called “nonmagnetic background” contribution), and ξ represents the short-range ion-core–ion-core interaction and is, therefore, sensitive to thermal volume expansion, while χ_P and χ_S are, respectively, the Pauli and Stoner spin susceptibilities. For Invar systems such as the ones under consideration, thermal expansion is negligible¹³ and hence $\Delta E(T)/E_0 \propto \chi_S^{-1}(T)$. Though a mean-field description is not valid in the critical region, we explored the possibility of such a direct relation between the measured $\Delta E/E_0$ and the

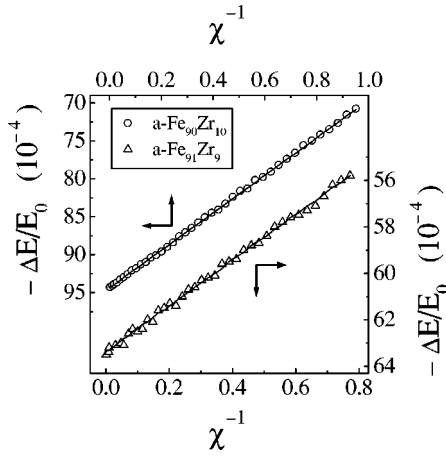


FIG. 5. $\Delta E/E_0$ versus χ^{-1} plots for $a\text{-Fe}_{90}\text{Zr}_{10}$ (open circles) and $a\text{-Fe}_{91}\text{Zr}_9$ (open triangles) alloys. The straight lines through the data represent the least-squares fits. The susceptibility data used to construct such plots are taken from Ref. 12.

previously published¹² *intrinsic* magnetic susceptibility²⁴ (i.e., the measured susceptibility χ_{meas} corrected for demagnetizing effects) $\chi(T)$ of the amorphous alloys with the same nominal composition as the present ones. A *linear* relationship between $\Delta E(T)/E_0$ and $\chi^{-1}(T)$ for temperatures in a narrow range above T_C is borne out clearly by the data presented in Fig. 5. In this context, the earlier claim²⁵ that $\Delta E(T)/E_0 \propto \chi_{meas}^{-1}(T)$ for $a\text{-Fe}_{90}\text{Zr}_{10}$ has to be treated with caution since the temperature variations of $\chi(T)$ and $\chi_{meas}(T)$ are widely different, particularly in the critical region; $\chi(T)$ *diverges* at T_C while $\chi_{meas}(T)$ remains *finite*.

In view of the above observation (Fig. 5), $\Delta E(T)/E_0$ data are analyzed in terms of the expression¹² for $\chi(T)$:

$$\left(\frac{\Delta E(T)}{E_0}\right) - \left(\frac{\Delta E(T_C)}{E_0}\right) = \Gamma^{-1} \epsilon^\gamma (1 + a_{\chi_1}^+ \epsilon^{\Delta_1} + a_{\chi_2}^+ \epsilon^{\Delta_2})^{-1}, \quad (8)$$

which includes the leading correction-to-scaling (CTS) terms and is valid in the ACR for $\epsilon > 0$. The same fitting procedure as that adopted earlier for sound velocity is followed and an elaborate range-of-fit analysis is carried out based on Eq. (8) by either including or excluding the CTS terms. The single-power-law fits, based on Eq. (8) with $a_{\chi_1}^+ = a_{\chi_2}^+ = 0$, do not reproduce the observed temperature variation of $\Delta E/E_0$ in the critical region as closely as the CTS fits (solid curves in Fig. 6) do, as is inferred from a substantially lower sum of the deviation squares in the latter case. The optimum values of the free fitting parameters T_C , γ , Γ^{-1} , $a_{\chi_1}^+$, and $a_{\chi_2}^+$ (with Δ_1 and Δ_2 fixed at^{9,10,21} $\Delta_1 = 0.11$ and $\Delta_2 = 0.55$) for the CTS fits are displayed in Table II and compared with the corresponding values obtained *directly* from the susceptibility data previously.¹² The presently determined values for the CTS amplitudes $a_{\chi_1}^+$, $a_{\chi_2}^+$ and critical exponent γ , though obtained via an *indirect* method, are in excellent agreement with those yielded earlier by susceptibility¹² and also with the most accurate theoretical estimate^{9,10} for γ for an ordered spin system with $d = n = 3$ (Table II).

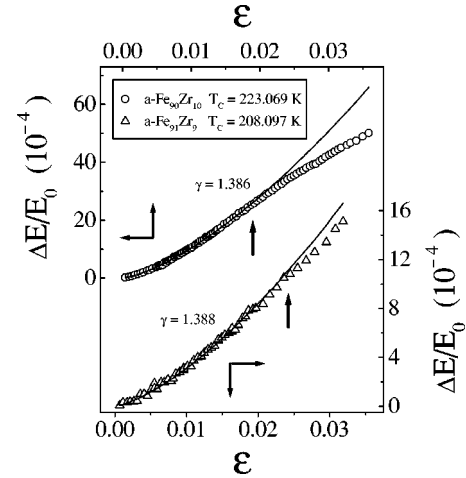


FIG. 6. Variation of $\Delta E/E_0$ with reduced temperature $\epsilon = (T - T_C)/T_C$ for $a\text{-Fe}_{90}\text{Zr}_{10}$ (open circles) and $a\text{-Fe}_{91}\text{Zr}_9$ (open triangles) alloys. The solid curves depict the least-squares fits to the $\Delta E/E_0$ data based on Eq. (8) of the text. The upward arrows indicate the temperatures that mark the upper bound of the asymptotic critical region beyond which the data start deviating from the fits.

The following observations can be made based on the data presented in Tables I and II. (i) The sound velocity and Young's modulus data yield the *same* value for T_C^+ for a given alloy composition, as demanded by the internal consistency between the two sets of data. (ii) The values of the critical exponents α^\pm and γ , together with the previously reported¹² value of the critical exponent β for spontaneous magnetization, satisfy the scaling equalities $\alpha^+ = \alpha^- \equiv \alpha$ and $\alpha + 2\beta + \gamma = 2$, valid for a second-order phase transition. (iii) The universal specific heat critical amplitude ratio A^+/A^- and the critical exponents α^\pm , γ possess values that tally well with those theoretically predicted^{9,10,22} for an isotropic $d = 3$, $n = 3$ spin system. Considering the fact that $a\text{-Fe}_{90}\text{Zr}_{10}$ and $a\text{-Fe}_{91}\text{Zr}_9$ are weak *itinerant-electron* ferromagnets,^{12,14,15} the observation (iii) that these alloys behave as an ordered $d = 3$ nearest-neighbor Heisenberg (*localized electron*) ferromagnet in the asymptotic critical region seems untenable. This apparent contradiction can be resolved as follows. The renormalization group (RG) calculations²⁶ on a d -dimensional spin system with an *isotropic* n -component order parameter and *long-range* attractive interactions decaying as $1/r^{(d+\sigma)}$ ($\sigma > 0$) with the interspin spacing r reveals that the critical exponents assume their *short-range* values for all d if $\sigma > 2$. For a $d = 3$, $n = 3$ spin system wherein spins are coupled through attractive interactions that *decay* faster than $1/r^5$, these RG calculations²⁶ predict the same critical behavior as that of a $d = 3$ nearest-neighbor Heisenberg ferromagnet. The observation (iii) thus asserts that the alloys in question are the experimental realizations of this RG prediction.

IV. SUMMARY

High-resolution Young's modulus and sound velocity data have been obtained on amorphous *Invar* $\text{Fe}_{90}\text{Zr}_{10}$ and $\text{Fe}_{91}\text{Zr}_9$ alloys over a wide temperature range that spans the

TABLE II. Parameters values pertaining to Eq. (8) of the text.

Alloy	Method	Fit range ($10^3 \epsilon$)	T_C^+ (K)	γ	Γ^{-1}	$a_{\chi_1}^+$	$a_{\chi_2}^+$
a -Fe ₉₀ Zr ₁₀	CTS	0.41–20	223.069(4)	1.386(2)	0.558(4)	−0.045(2)	−0.80(4)
	($\Delta E/E_0$)						
a -Fe ₉₁ Zr ₉	CTS	0.78–45	224.97(4)	1.390(5)	233(11)	−0.05(1)	−0.8(1)
	{ $\chi(T)$ }						
	CTS	0.69–25	208.097(8)	1.388(2)	0.168(2)	−0.045(2)	−0.80(1)
	($\Delta E/E_0$)						
	CTS	0.39–41	209.63(3)	1.383(4)	175(9)	−0.03(1)	−0.5(1)
	{ $\chi(T)$ }						
$d=3$				1.386(4)			
Heisenberg model ^a							

^aReferences 9 and 10.

critical region near the ferromagnetic-paramagnetic phase transition from the vibrating reed experiments. A linear relationship is found to hold between the magnetic contribution to Young's modulus, $\Delta E(T)/E_0$, and inverse magnetic susceptibility χ^{-1} in the critical region. This relationship permits as *accurate* a determination of the asymptotic critical exponent γ and the leading correction-to-scaling amplitudes for susceptibility from $\Delta E(T)/E_0$ data as is possible directly from the $\chi(T)$ data. The well-established proportionality between the magnetic contributions to sound velocity, $\Delta V(T)/V_0$, and specific heat, $C_M(T)$, has been used in obtaining accurate estimates for the universal critical amplitude ratio A^+/A^- and the asymptotic critical exponents α^\pm for specific heat from the $\Delta V(T)/V_0$ data. The values of α^\pm and γ , so obtained, along with the previously determined¹² magnitude of the critical exponent β , not only obey scaling equalities $\alpha^- = \alpha^+$ and $\alpha + 2\beta + \gamma = 2$ but also conform well with the corresponding theoretical estimates yielded by renormalization group calculations for an ordered isotropic $d=3$, $n=3$ spin system in which spins (atomic magnetic moments) interact with one another through an *attractive*

interaction which *decays faster* than $1/r^5$ with the interspin distance r . Finally, it should be emphasized that the critical amplitudes and exponents for susceptibility and specific heat have been obtained by an *indirect* method that exploits the *direct* relationships between the magnetic contribution to Young's modulus and inverse "zero-field" magnetic susceptibility, on the one hand, and between the magnetic contributions to sound velocity and specific heat, on the other.

ACKNOWLEDGEMENTS

One of the authors (K.B.) would like to thank Professor R. Srinivasan, Raman Research Institute, Bangalore, Dr. B.A. Dasannacharya, Professor Ajay Gupta, Dr. V. Ganesan, and N. Vijayakumar, Inter University Consortium for Department of Atomic Energy Facilities, Indore, and A.C. Thakurta, Center for Advanced Technology, Indore, for fruitful discussions. K.B. gratefully acknowledges the financial support received from the Council of Scientific and Industrial Research, New Delhi, India.

*Author to whom correspondence should be addressed. Electronic address: kaulsp@uohyd.ernet.in

¹Articles by M. Gottlieb, M. Garbuny, and C.K. Jones, and C.W. Garland in *Physical Acoustics*, edited by W.P. Mason and R.N. Thurston (Academic, New York, 1970), Vol. 7, pp. 1 and 51.

²I.K. Kamilov and Kh.K. Aliev, *Sov. Phys. Usp.* **41**, 865 (1998).

³B. Lüthi, T.J. Moran, and R.J. Pollina, *J. Phys. Chem. Solids* **31**, 1741 (1970).

⁴B. Lüthi and R.J. Pollina, *Phys. Rev. Lett.* **22**, 717 (1969).

⁵K. Kawasaki and A. Ikushima, *Phys. Rev. B* **1**, 3143 (1970).

⁶M. Barmatz and B. Golding, *Phys. Rev. B* **9**, 3064 (1974).

⁷M.E. Lines, *Phys. Rev.* **55**, 133 (1979).

⁸G.F. Hawkins, R.L. Thomas, and A.M. de Graaf, *J. Appl. Phys.* **50**, 1709 (1979).

⁹J.C. LeGuillou and J. Zinn-Justin, *Phys. Rev. B* **21**, 3976 (1980).

¹⁰S.G. Gorishny, S.A. Larin, and F.V. Tkachov, *Phys. Lett.* **101A**, 120 (1984).

¹¹P.D. Babu and S.N. Kaul, *J. Non-Cryst. Solids* **220**, 147 (1997); P.D. Babu, S.N. Kaul, L.F. Barquín, J.C. Gómez Sal, W.H. Kettler, and M. Rosenburg, *Int. J. Mod. Phys. B* **13**, 141 (1999).

¹²P.D. Babu and S.N. Kaul, *J. Phys.: Condens. Matter* **9**, 7189 (1997).

¹³K. Shirakawa, S. Ohnuma, M. Nose, and T. Masumoto, *IEEE Trans. Magn.* **MAG-16**, 910 (1980).

¹⁴S.N. Kaul, *Phys. Rev. B* **27**, 6923 (1983); *J. Phys.: Condens. Matter* **3**, 4027 (1991).

¹⁵S.N. Kaul and P.D. Babu, *J. Phys.: Condens. Matter* **10**, 1563 (1998).

¹⁶K. Shirakawa, T. Kaneko, M. Nose, S. Ohnuma, H. Fujimori, and T. Masumoto, *J. Appl. Phys.* **52**, 1829 (1981).

¹⁷K. Balakrishnan, Manmeet Kaur Marhas, Nandkishor L. Ghodke, V. Ganesan, and R. Srinivasan, *Rev. Sci. Instrum.* **68**, 3436 (1997).

¹⁸K. Balakrishnan, P.D. Babu, V. Ganesan, R. Srinivasan, and S.N.

- Kaul, J. *Magn. Mater.* (to be published).
- ¹⁹Y.P. Varshni, *Phys. Rev. B* **2**, 3952 (1970).
- ²⁰S.N. Kaul and M. Sambasiva Rao, *Phys. Rev. B* **43**, 11 240 (1991); *J. Phys.: Condens. Matter* **6**, 7403 (1994).
- ²¹T.C. Lubensky, *Phys. Rev. B* **11**, 3573 (1975); G. Grinstein and A. Luther, *ibid.* **13**, 1329 (1976).
- ²²V. Privman, P.C. Hohenberg, and A. Aharony, in *Phase Transitions and Critical Phenomena*, edited by C. Domb and J.L. Lebowitz (Academic, New York, 1991), Vol. 14, p. 1.
- ²³D.J. Kim, *Phys. Rep.* **171**, 129 (1988).
- ²⁴The *intrinsic* magnetic susceptibility, $\chi(T)$, data published in Ref. 12 have been obtained as follows. From the measured magnetization (M) versus external magnetic field (H_{ext}) isotherms (taken at fixed temperatures in the range $70 \text{ K} \leq T \leq T_C$ in fields up to 15 kOe), the modified Arrott [$M^{1/\beta}$ versus $(H/M)^{1/\gamma}$] plot (MAP) isotherms are constructed with the choice of the critical exponents β and γ for spontaneous magnetization and initial susceptibility, respectively, which makes the MAP isotherms a set of straight lines. The values of χ^{-1} at different temperatures are then computed from the intercepts on the abscissa [$(H/M)^{1/\gamma}$ axis] obtained by extrapolating high-field *linear* portions of the MAP isotherms for $T \geq T_C$ to $M^{1/\beta} = 0$ (note that $H = H_{ext} - 4\pi NM$, where N is the demagnetizing factor). The Curie temperature T_C marks the temperature for which linear MAP isotherm, when extrapolated to $H = 0$, passes through the origin.
- ²⁵S.H. Park, Y.H. Jeong, K. Nahm, and C.K. Kim, *Solid State Commun.* **92**, 645 (1994).
- ²⁶M.E. Fisher, S.K. Ma, and B.G. Nickel, *Phys. Rev. Lett.* **29**, 917 (1972).